ISSN 1674-1056
http://cpb.iphy.ac.cn
http://iopscience.iop.org/cpb
中国物理 B
Chinese Physics
中国物理
Chinese Physics B

Method of evaluating interface traps in Al_2O_3/AlGaN/GaN high electron mobility transistors

Si-Qin-Gao-Wa Bao(包斯琴高娃), Xiao-Hua Ma(马晓华), Wei-Wei Chen(陈伟伟), Ling Yang(杨凌), Bin Hou(侯斌), Qing Zhu(朱青), Jie-Jie Zhu(祝杰杰), Yue Hao(郝跃)

Citation: Chin. Phys. B . 2019, 28(6): 067304. **doi:** 10.1088/1674-1056/28/6/067304
Journal homepage: http://cpb.iphy.ac.cn; http://iopscience.iop.org/cpb

What follows is a list of articles you may be interested in

Theoretical analytic model for RESURF AlGaN/GaN HEMTs

Hao Wu(吴浩), Bao-Xing Duan(段宝兴), Luo-Yun Yang(杨珞云), Yin-Tang Yang(杨银堂)
Chin. Phys. B . 2019, 28(2): 027302. **doi:** 10.1088/1674-1056/28/2/027302

1.8-kV circular AlGaN/GaN/AlGaN double-heterostructure high electron mobility transistor

Sheng-Lei Zhao(赵胜雷), Zhi-Zhe Wang(王之哲), Da-Zheng Chen(陈大正), Mao-Jun Wang(王茂俊), Yang Dai(戴扬), Xiao-Hua Ma(马晓华), Jin-Cheng Zhang(张进成), Yue Hao(郝跃)
Chin. Phys. B . 2019, 28(2): 027301. **doi:** 10.1088/1674-1056/28/2/027301

Effect of gate length on breakdown voltage in AlGaN/GaN high-electron-mobility transistor

Jun Luo(罗俊), Sheng-Lei Zhao(赵胜雷), Min-Han Mi(宓珉瀚), Wei-Wei Chen(陈伟伟), Bin Hou(侯斌), Jin-Cheng Zhang(张进成), Xiao-Hua Ma(马晓华), Yue Hao(郝跃)
Chin. Phys. B . 2016, 25(2): 027303. **doi:** 10.1088/1674-1056/25/2/027303

Trap states induced by reactive ion etching in AlGaN/GaN high-electron-mobility transistors

Luo Jun, Zhao Sheng-Lei, Mi Min-Han, Hou Bin, Yang Xiao-Lei, Zhang Jin-Cheng, Ma Xiao-Hua, Hao Yue
Chin. Phys. B . 2015, 24(11): 117305. **doi:** 10.1088/1674-1056/24/11/117305

Transport mechanism of reverse surface leakage current in AlGaN/GaN high-electron mobility transistor with SiN passivation

Zheng Xue-Feng, Fan Shuang, Chen Yong-He, Kang Di, Zhang Jian-Kun, Wang Chong, Mo Jiang-Hui, Li Liang, Ma Xiao-Hua, Zhang Jin-Cheng, Hao Yue
Chin. Phys. B . 2015, 24(2): 027302. **doi:** 10.1088/1674-1056/24/2/027302

Method of evaluating interface traps in Al_2O_3/AlGaN/GaN high electron mobility transistors*

Si-Qin-Gao-Wa Bao(包斯琴高娃)[1,2,3], Xiao-Hua Ma(马晓华)[1,2,†], Wei-Wei Chen(陈伟伟)[4], Ling Yang(杨凌)[1,2], Bin Hou(侯斌)[1,2], Qing Zhu(朱青)[1,2], Jie-Jie Zhu(祝杰杰)[1,2], and Yue Hao(郝跃)[2]

[1] *School of Advanced Materials and Nanotechnology, Xidian University, Xi'an* 710071, *China*
[2] *Key Laboratory of Wide Band-Gap Semiconductor Materials and Devices, School of Microelectronics, Xidian University, Xi'an* 710071, *China*
[3] *School of Science, Inner Mongolia University of Technology, Hohhot* 010051, *China*
[4] *China Academy of Space Technology (Xi'an), Xi'an* 710071, *China*

(Received 20 November 2018; revised manuscript received 2 April 2019; published online 8 May 2019)

In this paper, the interface states of the AlGaN/GaN metal–insulator–semiconductor (MIS) high electron mobility transistors (HEMTs) with an Al_2O_3 gate dielectric are systematically evaluated. By frequency-dependent capacitance and conductance measurements, trap density and time constant at Al_2O_3/AlGaN and AlGaN/GaN interface are determined. The experimental results reveal that the density of trap states and the activation energy at the Al_2O_3/AlGaN interface are much higher than at the AlGaN/GaN interface. The photo-assisted capacitance-voltage measurements are performed to characterize the deep-level traps located near mid-gap at the Al_2O_3/AlGaN interface, which indicates that a density of deep-level traps is lower than the density of the shallow-level states.

Keywords: AlGaN/GaN, HEMTs, interface traps, frequency-dependent *C*–*V* measurements, photo-assisted *C*–*V* measurements

PACS: 73.61.Ey, 73.40.Kp, 73.50.Gr **DOI:** 10.1088/1674-1056/28/6/067304

1. Introduction

When the gate is driven with a forward bias,[1–3] GaN-based metal–insulator–semiconductor (MIS) high electron mobility transistor (HEMT) can effectively suppress the gate leakage current and enlarge the gate voltage swing and, therefore, it is attractive to high-voltage and high-power applications. Among all the commonly used dielectric materials such as Si_3N_4,[4–6] SiO_2,[7–9] Al_2O_3,[10–13] HfO_2,[14–16] ZrO_2,[17] and Ta_2O_5,[18–20] the Al_2O_3 is one of the leading candidates for gate insulator in GaN-based devices due to its large band-gap (7 eV–9 eV), high dielectric constant (8–10), and high breakdown field (10 MV/cm).[21–23] In Table 1 the high-*k* dielectric material properties are summarized, such as band-gap, dielectric constant and breakdown field. Combined with the gate recessed process, Al_2O_3/AlGaN/GaN metal–oxide–semiconductor (MOS) HEMTs with an output power density of 13 W/mm and the associated power added efficiency (PAE) of 73% at 4-GHz frequency have been achieved in our group.[24] However, a large number of interface traps exist in the present GaN-based MIS HEMTs[25–27] and cause various operational stability and reliability problems, particularly for the threshold fluctuations.[28–30] In order to realize the long-term reliability and wide commercial deployment, the evaluation of the interface states is of vital importance.

Frequency-dependent capacitance and conductance measurements have been widely implemented to analyze the trap states in GaN-based HEMTs.[31–35] Since the deep trap states cannot respond to the AC signal during the *C*–*V* measurements,[36] only shallow trap states can be detected by using this method. Recently, the photo-assisted *C*–*V* method has been proved effective in activating deep trap states at the insulator/AlGaN interface.[37,38] In this paper, trap states near the conduction band edge at the Al_2O_3/AlGaN and AlGaN/GaN interfaces are characterized by performing the frequency-dependent *C*–*V* measurements, and the near mid-gap trap states at the Al_2O_3/AlGaN interface are analyzed by the photo-assisted *C*–*V* technique.

Table 1. Comparison of high-*k* dielectric material properties

High-*k* dielectric	Band gap/eV	Dielectric constant	Breakdown field/(MV/cm)
Si_3N_4[4–6]	4–6	5–7	5–7
SiO_2[7–9]	9	4	8–9
Al_2O_3[21–23]	7–9	8–10	10
HfO_2[14–16]	4.5–6	20	6–8
ZrO_2[17]	5–6	17	7.4
Ta_2O_5[18–20]	4–5	20	4

2. Devices and experiments

The AlGaN/GaN epitaxial structure was grown by the metal organic chemical vapor deposition (MOCVD) on a

*Project supported by the Key Program of National Natural Science Foundation of China (Grant Nos. 61334002 and 61634005) and the National Natural Science Foundation of China (Grant Nos. 61604114 and 61704124).

†Corresponding author. E-mail: xhma@xidian.edu.cn

© 2019 Chinese Physical Society and IOP Publishing Ltd

(0001) sapphire substrate. The epitaxial growth was initiated with an AlN nuclear layer followed by a 1.3-μm unintentionally doped (UID) GaN layer. This was followed by a 1-nm-thick AlN interlayer and a 22-nm-thick $Al_{0.3}Ga_{0.7}N$ barrier layer. Finally, a 1-nm-thick GaN cap-layer was deposited on the surface of AlGaN barrier. The device fabrication started with mesa isolation, which was performed by reactive ion etching (RIE) with an etch-depth of 200 nm. Ohmic contacts consisting of Ti/Al/Ni/Au were annealed in a nitrogen ambient at 850 °C for 30 s, yielding a contact resistance of 0.5 Ω·mm. Then a 15-nm-thick Al_2O_3 gate dielectric was deposited by an atomic layer deposition (ALD) system at 300 °C with trimethylaluminum (TMA) and ozone (O_3) serving as the precursors. Afterwards, the gate contacts of Ni/Au/Ni were evaporated on the Al_2O_3 layer.

Fat-HEMTs with a gate length of 50 μm and gate width of 100 μm were fabricated. The gate-to-source and gate-to-drain spacing of each device are both 3.0 μm. Figure 1 shows the cross section and Schottky characteristics of the fabricated Al_2O_3/AlGaN/GaN HEMT. The reverse leakage current was below 1 nA and the forward bias can reach a value as high as +8 V, demonstrating a low reverse leakage and a high forward gate voltage withstanding. The *C*–*V* measurements were performed by Keithley 4200SCS semiconductor analyzer with a frequency range from 10 kHz to 10 MHz. For the photo-assisted *C*–*V* measurement, light emitting diodes (LED) with different wave lengths but the same light intensity were used.

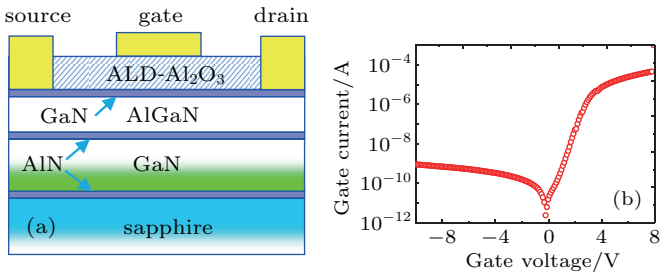


Fig. 1. (a) Cross-section and (b) Schottky characteristics of the fabricated Al_2O_3/AlGaN/GaN HEMT.

3. Results and discussion

In this section, trap states near the conduction band edge at the Al_2O_3/AlGaN and AlGaN/GaN interface are investigated by the frequency-dependent *C*–*V* measurements. And, the near mid-gap trap states at the Al_2O_3/AlGaN interface are analyzed by the photo-assisted *C*–*V* technique.

3.1. Frequency-dependent *C*–*V* measurements

Figure 2 shows the typical capacitance–voltage (C_m–V) and conductance–voltage (G_m–V) curves of the Al_2O_3/AlGaN/GaN HEMTs at given frequencies from 50 kHz to 1 MHz. The measurement equivalent circuit is modeled as the parallel-connected capacitance C_m and conductance G_m as indicated in the inset of Fig. 2. Two capacitance plateaus can be clearly seen, featuring two sharp transitions from accumulation to depletion at about 3.0 V and −3.4 V. The capacitance plateau in the forward bias region represents the Al_2O_3 dielectric capacitance ($C_{Al_2O_3}$), and the capacitance plateau in the reverse bias region corresponds to the total capacitance (C_{total}) of the Al_2O_3 dielectric and the AlGaN barrier. The significant frequency dispersion of the C_m and G_m at the two step-like profiles can be observed in Fig. 2 due to a number of interface traps at both the Al_2O_3/AlGaN and AlGaN/GaN interface.[12,23,25] When the gate is driven with a forward bias, the AlGaN/GaN heterojunction interface traps are far below the Fermi level, thus only the Al_2O_3/AlGaN interface traps can respond to the ac signal. Similarly, in the reverse bias region, only the AlGaN/GaN interface traps are able to make a contribution to the frequency dispersion, whereas the response of the Al_2O_3/AlGaN interface traps is excluded. Therefore, the traps at the Al_2O_3/AlGaN and the AlGaN/GaN interface can be characterized separately.

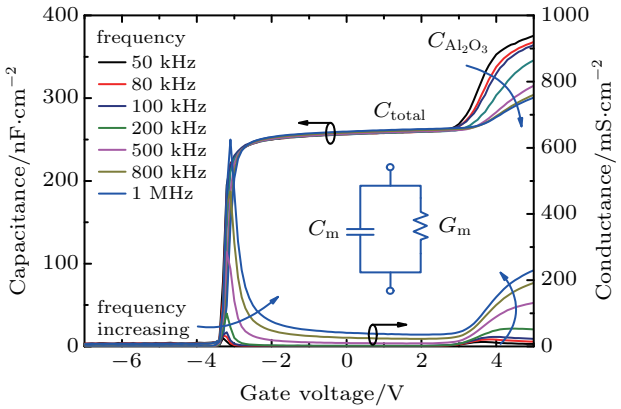


Fig. 2. Typical C_m–V and G_m–V characteristics of the Al_2O_3/AlGaN/GaN HEMTs at given frequencies from 50 kHz to 1 MHz.

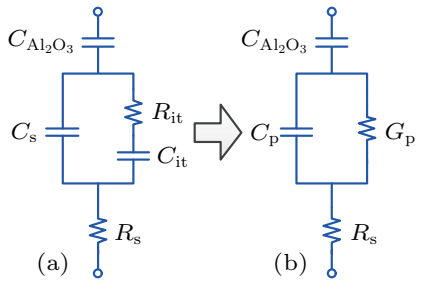


Fig. 3. (a) Equivalent circuit model used to extract trap parameters considering the Al_2O_3/AlGaN interface trap and (b) further simplified circuit.

The trapping and de-trapping process of Al_2O_3/AlGaN interface trap states can be modeled as a combination of series-connected trap-related resistance (R_{it}) and capacitance (C_{it}) with a parallel-connected semiconductor capacitance (C_s). With the response of AlGaN/GaN interface traps excluded, the equivalent circuit in the forward bias region can be plotted as shown in Fig. 3(a). The semiconductor capacitance C_s represents the total capacitance of the AlGaN barrier layer and the

GaN buffer layer. The capacitance of the GaN cap layer and the AlN interlayer are neglected since they are very thin. Besides, the parasitic resistance R_s is also included in the circuit. This full equivalent circuit can be transformed into a simplified model as shown in Fig. 3(b). In the circuit, the electrical behavior of Al_2O_3/AlGaN interface trap state is modeled by parallel-connected conductance G_p and capacitance C_p.

Assuming that energy level, trap state time constant τ_T, and trap density D_T can be evaluated by fitting the parallel conductance G_p/ω as a function of the radial frequency ($\omega = 2\pi f$) according to the following equation[31]

$$\frac{G_p}{\omega} = \frac{q\omega\tau_T D_T}{1+(\omega\tau_T)^2}. \tag{1}$$

The parallel conductance G_p/ω can be obtained from the measured capacitance C_m and conductance G_m by from the following relation[25]

$$\frac{G_p}{\omega} = \frac{\omega G_m C_{Al_2O_3}^2}{G_m^2 + \omega^2\left(C_{Al_2O_3} - C_m\right)^2}. \tag{2}$$

For the AlGaN/GaN interface traps, the trap state time constant τ_T and trap density D_T can be obtained using the same method, *i.e.*, using C_{total} to replace $C_{Al_2O_3}$ in Fig. 3 and Eq. (2). The value of $C_{Al_2O_3}$ and C_{total} can be explicitly determined from the plateaus in C_m–V curve in Fig. 2.

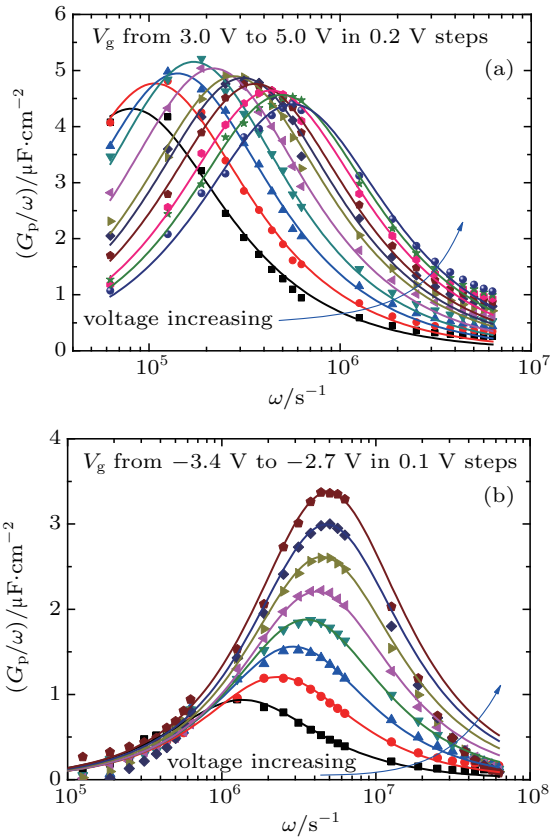


Fig. 4. Plots of parallel conductance *versus* radial frequency at selected gate bias V_g ranging (a) from 3.0 V to 5.0 V in steps of 0.2 V and (b) from −3.4 V to −2.7 V in steps of 0.1 V. Solid line curves are fitting curves to experimental data.

Based on the experimental results in Fig. 2, two ranges of gate bias are selected in the vicinity of respective threshold voltage (around 3.0 V and −3.4 V) to conduct the frequency-dependent capacitance and conductance measurement, where the frequency dispersion is obvious. Figure 4 shows the plots of G_p/ω *versus* radial frequency at selected gate biases, obtained according to Eq. (2). Each plot of G_p/ω *versus* ω gives a peak for a corresponding gate bias, implying that the contributions of interface traps near the conduction band edge possess different values of time constant (τ_T) and density (D_T). The fitting curves based on Eq. (1) are shown as full lines in Fig. 4, from which the trap state time constant τ_T and trap density D_T at each gate bias can be extracted directly.

Figure 5(a) shows the plots of trap state time constant (τ_T) *versus* gate voltage evaluated from the G_p/ω measurement. It can be seen from the figure that the values of time constant (τ_T) almost exponentially decrease with gate voltage increasing from 12.36 μs to 1.77 μs for the Al_2O_3/AlGaN interface traps and from 0.73 μs to 0.20 μs for the AlGaN/GaN interface respectively. It should be noted that the trap states at the Al_2O_3/AlGaN interface are mainly slow traps, and a time constant is about one order of magnitude larger than that at the AlGaN/GaN interface. The trap state density as a function of the corresponding energy level below the conduction band is plotted in Fig. 5(b). The trap state energy E_T is derived from the following expression:

$$\tau_T = (\sigma_T N_c v_T)^{-1} \exp\left(\frac{E_T}{kT}\right), \tag{3}$$

where capture cross section of trap state $\sigma_T = 3.4\times10^{-15}$ cm^2, the density of states in the conduction band $N_c = 4.3\times10^{14}\times T^{3/2}$ cm^{-3}, and the average thermal velocity of the carriers $v_T = 2.6\times10^7$ cm/s have proved valid.[39] The trap density D_T apparently decreasing from 4.21×10^{13} cm^{-2}·eV^{-1} to 1.17×10^{13} cm^{-2}·eV^{-1} can be seen, when the trap energy E_T increases from 0.27 eV to 0.31 eV for the AlGaN/GaN interface traps. The trap density D_T is dependent on trap energy E_T, and the lower the trap energy E_T, the higher the trap density D_T is. It indicates that the trap with lower trap energy can easily capture electrons. The traps at the Al_2O_3/AlGaN interface are deeper, located in a range of 0.33 eV–0.38 eV below the conduction band edge. Comparing with the AlGaN/GaN interface, the trap density keeps a much higher value in the whole trap energy range of about 5.39 cm^{-2}·eV^{-1}–5.49×10^{13} cm^{-2}·eV^{-1}. The trap density D_T is independent of trap energy E_T, indicating that the ability to capture electron is independent of trap energy E_T.

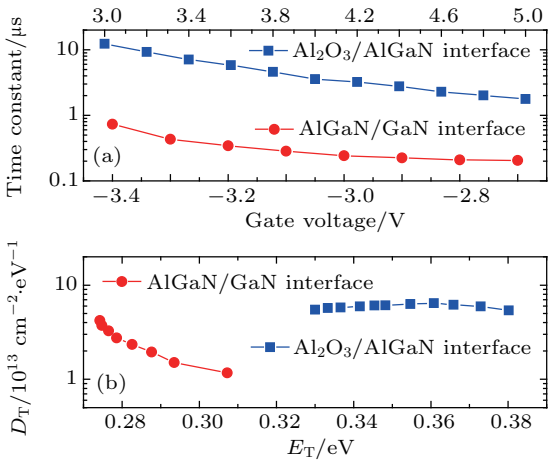


Fig. 5. (a) Plot of experimentally extracted trap state time constant *versus* (a) gate voltage and (b) trap density *versus* derived trap energy for Al_2O_3/AlGaN and AlGaN/GaN interface traps.

3.2. Photo-assisted *C–V* measurements

Due to the limited frequency range (10 kHz to 10 MHz) utilized in this paper, only the interface traps located in the range from 0.21 eV to 0.39 eV can be detected according to Eq. (3). In order to investigate the deeper interface states near the mid-gap, photo-assisted *C–V* measurement is introduced. Figure 6 shows the typical variation of capacitance with time increasing from 0 s to 1100 s at 100 kHz under light illumination. During the measurement the gate voltage is kept at a constant value of −4.5 V and the light source with a wave length of 465 nm is turned on and off alternately. It can be observed that the capacitance increases sharply right after the light has been turned on and the enhancement in the capacitance can persist for a long period after the light has been turned off, which is very similar to the persistent photoconductivity (PPC) effect.[40] Under the light illumination, the electrons are photo-excited from the deep-level donors and cause the capacitance to quickly increase. Since the recombination of electrons and ionized deep-level donors is prevented from happening by the local potential barrier, the capacitance exhibits a slower decrease after the light excitation has ended.

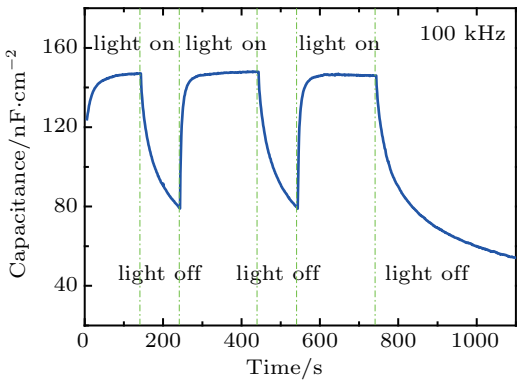


Fig. 6. Variation of capacitance with time from 0 s to 1100 s at 100 kHz under light illumination. During measurement, gate voltage is kept constant and light source with wave length of 465 nm is turned on and off alternately.

Based on the capacitance transient properties, photo-assisted *C–V* measurements are performed. Before the light illumination the *C–V* hysteresis property of the device is measured from −8 V to 5 V in dark at a frequency of 100 kHz. Then the sample is illuminated for 60 s while the bias is kept at −8 V, and the trapped electrons from deep-level trap states are emitted as depicted in Fig. 7(a). Afterwards, the light is turned off and the device is swept from −8 V towards 5 V immediately. In the present investigation, the *C–V* curves are recorded under the wave length of incident light varying from 520 nm to 400 nm. As shown in Fig. 7(b), the sharp transition at the reverse bias region exhibits a clear parallel shift towards the negative bias direction after light illumination, while the shift in the forward bias region is less apparent. Since the light illumination with the shorter wave length can cause the relatively deeper states to ionize, the resulting gate voltage negative shift is also larger. The amount of the voltage shift increases from 1.0 V to 2.4 V as the wave length of the incident light decreases from 520 nm to 400 nm, which can be seen in Fig. 7(b).

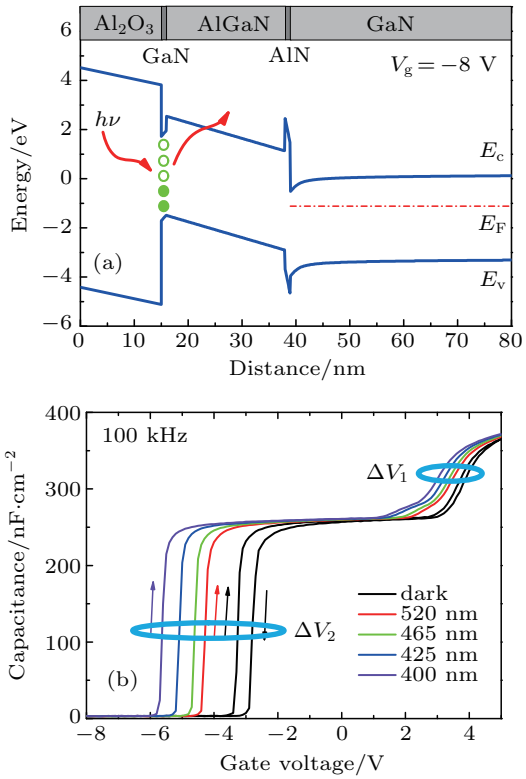


Fig. 7. Plots of (a) photo-assisted electron emission at the Al_2O_3/AlGaN interface and (b) typical *C–V* characteristics before and after light illumination.

The photon illumination with the higher energy causes the interface states to ionize in a wider energy. This results in a larger number of photo-ionized interface states, leading to the larger voltage shift in *C–V* curves as shown in Fig. 7. The state density of the near mid-gap traps can be estimated by using the difference between two voltage shifts with different wave lengths, ΔV_2, from the following equation[38]

$$D_{\rm it}(E = E_{\rm AV}) = \frac{C_{\rm total} \cdot \Delta V_2}{q \cdot \Delta h\nu}, \tag{4}$$

where C_{total} is the series capacitance of Al_2O_3 and AlGaN, $\Delta h\nu$ is the difference between two photo energies ($h\nu_2 - h\nu_1$), and E_{AV} is the average activation energy ($h\nu_1 + \Delta h\nu$ /2). The capacitance C_{total} can be obtained from Fig. 2, and the photo energy can be calculated from $h\nu = \text{hc}/\lambda$. As shown in Fig. 8, a trap density D_{it} varying from 1.83×10^{12} cm^{-2}·eV^{-1} to 4.61×10^{12} cm^{-2}·eV^{-1} located at E_{AV} of 2.53 eV–3.01 eV below the conduction band edge is derived. It is considered that the deep trap sites which are located at about 2.53 eV–3.01 eV from the conduction band edge are attributed to the GaN oxidation due to O_3 plasma. According to previous studies,[41–45] vacancy-type defects such as nitrogen vacancy (V_N) and gallium vacancy (V_{Ga}) are located around 0.24 eV and 2.62 eV from the conduction band edge, respectively. Furthermore, oxygen at a nitrogen site (O_N) and its complex with V_{Ga} (V_{Ga}–O_N) are located around 0.5 eV and 2.3 eV–3.3 eV from the conduction band edge, respectively. Therefore, the deep trap state due to GaN oxidation when using O_3 plasmaare possibly attributed to vacancy-type defects such as V_{Ga} and V_{Ga}–O_N. Comparing with Fig. 5, it can be seen that the interface states' density near mid-gap states is much lower than the interface states' density closer to conduction band edge. However, a significant threshold voltage shift (in the reverse bias region) can be induced by these near mid-gap interfaces as plotted in Fig. 7(b).

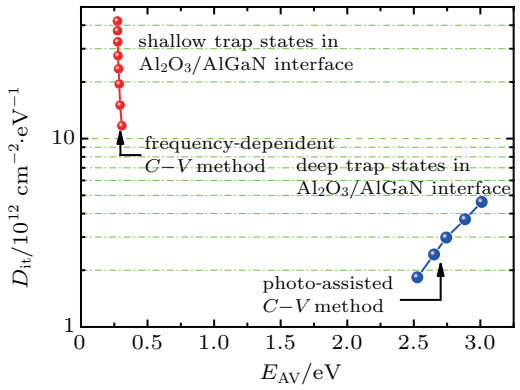


Fig. 8. Plots of experimentally extracted trap density *versus* trap energy for Al_2O_3/AlGaN interface traps, obtained by the photo-assisted *C–V* measurements and frequency-dependent *C–V* method.

4. Conclusions

In this work, the interface states of the Al_2O_3/AlGaN/GaN MOS-HEMTs are evaluated by frequency-dependent conductance analysis, in conjunction with photo-assisted *C–V* measurements. A distribution of the trap density from 4.21×10^{13} cm^{-2}·eV^{-1} to 1.17×10^{13} cm^{-2}·eV^{-1} with the trap energy ranging from 0.27 eV to 0.31 eV is yielded at the AlGaN/GaN interface. Nevertheless, the detected Al_2O_3/AlGaN interface states are deeper and have a high density of 5.39 cm^{-2}·eV^{-1}–5.49×10^{13} cm^{-2}·eV^{-1}, located at 0.33 eV–0.38 eV below the conduction band edge. In order to detect the deeper interface states at the Al_2O_3/AlGaN interface, the photo-assisted *C–V* analysis is performed and a low trap density of 1.83×10^{12} cm^{-2}·eV^{-1} to 4.61×10^{12} cm^{-2}·eV^{-1} located at E_{AV} of 2.53 eV–3.01 eV below the conduction band edge is derived. Although the density of deeper interface states at the Al_2O_3/AlGaN interface is much lower than the density of shallower interface states, it can induce significant threshold voltage instability.

References

[1] Hove M V, Kang X, Stoffels S, Wellekens D, Ronchi N, Venegas R, Geens K and Decoutere S 2013 *IEEE Trans. Electron. Dev.* **60** 3071
[2] Choi W, Seok O, Ryu H, Cha H Y and Seo K S 2014 *IEEE Electron Dev. Lett.* **35** 175
[3] Seo D W, Choi H G, Twynam J, Kim K M, Yim J S, Moon S W, Jung S, Lee J and Roh S D 2014 *IEEE Electron Dev. Lett.* **35** 446
[4] Fagerlind M, Allerstam F, Sveinbjornsson E O, Rorsman N, Kakanakova-Georgieva A, Lundskog A, Forsberg U and Janzen E 2010 *J. Appl. Phys.* **108** 014508
[5] Oka T and Nozawa T 2008 *IEEE Electron Dev. Lett.* **29** 668
[6] Swenson B L and Mishra U K 2009 *J. Appl. Phys.* **106** 064902
[7] Kordos P, Heidelberger G, Bernat J, Fox A, Marso M and Luth H 2005 *Appl. Phys. Lett.* **87** 143501
[8] Niiyama Y, Shinagawa T, Ootomo S, Kambayashi H, Nomura T and Yoshida S 2007 *Phys. Stat. Sol. (a)* **204** 2032
[9] Huang W, Khan T and Chow T P 2006 *IEEE Electron Dev. Lett.* **27** 796
[10] Kanamura M, Ohki T, Kikkawa T, Imanishi K, Imada T, Yamada A and Hara N 2010 *IEEE Electron Dev. Lett.* **31** 189
[11] Hashizume T, Ootomo S and Hasegawa H 2003 *Appl. Phys. Lett.* **83** 2952
[12] Yang S, Tang Z, Wong K Y, Lin Y S, Liu C, Lu Y, Huang S and Chen K J 2013 *IEEE Electron Dev. Lett.* **34** 1497
[13] Chu R, Corrion A, Chen M, Li R, Wong D, Zehnder D, Hughes B and Boutros K 2011 *IEEE Electron Dev. Lett.* **32** 632
[14] Tian F and Chor E F 2010 *J. Electrochem. Soc.* **157** H557
[15] Liu C, Chor E F and Tan L S 2006 *Appl. Phys. Lett.* **88** 173504
[16] Hayashi Y, Kishimoto S and Mizutani T 2010 *Solid-State Electron.* **54** 1451
[17] Ye G, Wang H, Arulkumaran S, Ng G I, Hofstetter R, Li Y, An, M J, Ang K S, Maung Y K T and Foo S C 2013 *Appl. Phys. Lett.* **103** 142109
[18] Deen D, Storm D, Meyer D, Katzer D S, Bass R, Binari S and Gougousi T 2011 *Phys. Status Solidi C* **8** 2420
[19] Kikkawa T, Makiyama K, Ohki T, Kanamura M, Imanishi K, Hara N and Joshin K 2009 *Phys. Status Solidi A* **206** 1135
[20] Deen D A, Storm D F, Bass R, Meyer D J, Katzer D S, Binari S C, Lacis J W and Gougousi T 2011 *Appl. Phys. Lett.* **98** 023506
[21] Ye P D, Yang B, Ng K K, Bude J, Wilk G D, Halder S and Hwang J C M 2005 *Appl. Phys. Lett.* **86** 063501
[22] Liu Z H, Ng G I, Arulkumaran S, Maung Y K T, Teo K L, Foo S C and Sahmuganathan V 2009 *Appl. Phys. Lett.* **95** 223501
[23] Mizue C, Hori Y, Miczek M and Hashizume T 2011 *Jpn. J. Appl. Phys.* **50** 021001
[24] Hao Y, Yang L, Ma X H, Ma J G, Cao M Y, Pan C Y, Wang C and Zhang J C 2011 *IEEE Electron Dev. Lett.* **32** 626
[25] Ma X H, Zhu J J, Liao X Y, Yue T, Chen W W and Hao Y 2013 *Appl. Phys. Lett.* **103** 033510
[26] Long R D, Jackson C M, Yang J, Hazeghi A, Hitzman C, Majety S, Arehart A R, Nishi Y, Ma T P, Ringel S A and Mclntyre P C 2013 *Appl. Phys. Lett.* **103** 201607
[27] Hung T H, Park P S, Krishnamoorthy S, Nath D N and Rajan S 2014 *IEEE Electron Dev. Lett.* **35** 312
[28] Johnson D W, Lee R T P, Hill R J W, Wong M H, Bersuker G, Piner E L, Kirsch P D and Harris H R 2013 *IEEE Trans. Electron. Dev.* **60** 3197

[29] Tapajna M, Jurkovic M, Valik L, Hascik S, Gregusova D, Brunner F, Cho E M and Kuzmik J 2013 *Appl. Phys. Lett.* **102** 243509
[30] Lu Y, Yang S, jiang Q, Tang Z, Li B and Chen K J 2013 *Phys. Status Solidi C* **10** 1397
[31] Miller E J, Dang X Z, Wieder H H, Asbeck P M, Yu E T, Sullivan G J and Redwing J M 2000 *J. Appl. Phys.* **87** 8070
[32] Stoklas R, Gregusova D, Novak J, Vescan A and Kordos P 2008 *Appl. Phys. Lett.* **93** 124103
[33] Gregusova D, Stoklas R, Mizue C, Hori Y, Novak J, Hashizume T and Kordos P 2010 *J. Appl. Phys.* **107** 106104
[34] Kordos P, Stoklas R, Gregusova D, Gazi S and Novak J 2010 *Appl. Phys. Lett.* **96** 013505
[35] Zhu J J, Ma X H, Xie Y, Hou B, Chen W W, Zhang J C and Hao Y 2015 *IEEE Trans. Electron. Dev.* **62** 512
[36] Ma X H, Chen W W, Hou B, Zhang K, Zhu J J, Zhang J C, Zheng X F and Hao Y 2014 *Appl. Phys. Lett.* **104** 093504
[37] Hori Y, Yatabe Z and Hashizume T 2013 *J. Appl. Phys.* **114** 244503
[38] Yatabe Z, Hori Y, Ma W C, Asubar J T, Akazawa M, Sato T and Hashizume T 2014 *Jpn. J. Appl. Phys.* **53** 100213
[39] Zhang K, Xue J S, Cao M Y, Yang L Y, Chen Y H, Zhang J C, Ma X H and Hao Y 2013 *J. Appl. Phys.* **113** 174503
[40] Arslan E, Butun S, Lisesivdin S B, Kasap M, Ozcelik S and Ozbay E 2008 *J. Appl. Phys.* **103** 103701
[41] Arehart A R, Corrion A, Poblenz C, Speck J S, Mishra U K and Ringel S A 2008 *Appl. Phys. Lett.* **93** 112101
[42] Johnstone D 2007 *Proc. SPIE*, December 16–18, 2007, Gifu, Japan, 64730L
[43] Elsner J, Jones R, Heggie M I, Sitch P K, Haugk M, Frauenheim T, Oberg S and Briddon P R 1998 *Phys. Rev. B* **58** 12571
[44] Chua S J, Choi H W, Zhang J and Li P 2001 *Phys. Rev. B* **64** 205302
[45] Puzyrev Y S, Roy T, Beck M, Tuttle B R, Schrimpf R D, Fleetwood D M and Pantelides S T 2011 *J. Appl. Phys.* **109** 034501